Environment International 143 (2020) 105884

Contents lists available at ScienceDirect

Environment International

journal homepage: www.elsevier.com/locate/envint

Semi-probabilistic coastal flood impact analysis: From deterministic hazards to multi-damage model impacts

Enrico Duo[a,*], Tomas Fernández-Montblanc[a,b], Clara Armaroli[c]

[a] Department of Physics and Earth Sciences, University of Ferrara, Via Saragat 1, 44122 Ferrara, Italy
[b] Department of Earth Sciences, International Campus of Excellence of the Sea (CEI·MAR), University of Cádiz, Avda. República Saharaui, 11510 Puerto Real, Cádiz, Spain
[c] Scuola Universitaria Superiore IUSS Pavia, Piazza della Vittoria 15, 27100 Pavia, Italy

ARTICLE INFO

Handling editor: Zhen (Jason) He

Keywords:
Relative sea level rise
Flooding
Damage
Extreme events
Stavanger
Norway

ABSTRACT

Coastal flood impact assessments are important tools for risk management and are performed by combining the hazard component with the vulnerability of exposed assets, to quantify consequences (or impacts) in terms of relative or absolute (e.g. financial) damage. The process generates uncertainties that should be taken into account for the correct representation of the consequences of floods. This study presents a coastal flood impact application at the spatial level of the Stavanger municipality (Norway), based on a multi-damage model approach able to represent impacts, and their overall uncertainty. Hazard modelling was performed using the LISFLOOD-FP code, taking into account historical extreme water level events (1988–2017) and relative sea level rise scenarios. Direct impacts were calculated in the form of relative and financial damage for different building categories, using flood damage curves. The results showed that the expected impacts are fewer than 50 flooded receptors and less than €1 million in damage in the current sea level scenario. The impacts could double by the end of the century, considering the most optimistic relative sea level scenario. The results were discussed considering the limitations of the approach for both hazard and impact modelling, that will be improved in future implementations. The outcome of this study may be useful for cost–benefit analyses of mitigation actions and local-scale plans for adaptation.

1. Introduction

The Sendai Framework for Disaster Risk Reduction emphasises the importance of understanding disaster risk as a basis to tackle current and future risk-related management challenges (Poljanšek et al., 2017). A correct understanding means, first of all, being able to fully quantify risk, from hazard to impact. To understand risks, current and future scenarios should be considered, including the possible effects of the ongoing climate crisis, as well as the future development of the areas at risk from a socio-economic viewpoint. Coastal flood risks, in particular, are expected to increase by more than two orders of magnitude by the end of the current century, as a consequence of rising (extreme) sea levels and socio-economic coastal development (Vousdoukas et al., 2018b).

Interest in coastal risk management has grown exponentially in Europe in recent decades, mainly because of the occurrence of major high–impact events (e.g. Cyclone Xynthia in France in 2010), rising political commitment (e.g. UN Hyogo and Sendai Frameworks; EU Floods Directive 2007/60/EC), and increasing awareness of the climate emergency. Regional and national contexts (e.g. political commitment, prioritization of resources, socio-economic aspects, etc..) - in addition to the complexity of the physical phenomena, the processes that cause damage to assets, and the generalised lack of recorded impacts for marine events - lead to fewer coastal flood impact assessments than riverine ones in terms of number of studies (i.e. number of papers in the scientific literature). For instance, there are more coastal risk assessment studies for The Netherlands rather than Italy, compared to fluvial ones.

Flood impact assessments are of foremost importance in support of prevention and preparedness activities to be implemented by regional and local coastal managers. Risks can be assessed at the regional level to prioritise resources for risk management (e.g. Armaroli and Duo, 2018; Armaroli et al., 2019), or at the local level to quantify the effects of disaster risk reduction measures (e.g. Sanuy et al., 2018) in the framework of integrated coastal risk reduction strategies (Barquet and Cumiskey, 2018). Flood risk quantification is also an important aspect for emergency/operational tasks (Molinari et al., 2013; Dottori et al., 2017), but these types of applications are still at the experimental level

* Corresponding author.
E-mail addresses: duonrc@unife.it (E. Duo), frntms@unife.it (T. Fernández-Montblanc), clara.armaroli@iusspavia.it (C. Armaroli).

https://doi.org/10.1016/j.envint.2020.105884
Received 26 February 2020; Received in revised form 15 May 2020; Accepted 9 June 2020
Available online 30 June 2020

or too simplified, and potential impacts are roughly quantified considering only hazard and exposed elements (e.g. Harley et al., 2016).

Risk assessments should be performed by combining the hazard component with the vulnerability of the exposed assets (or receptors) (Poljanšek et al., 2017) to quantify consequences (or impacts) in terms of relative or absolute (e.g. financial) damage. When such studies are implemented at the local scale, it is possible to perform detailed analysis at the receptor' scale (e.g. the built environment; Sanuy et al., 2018). This means that, besides the computation of the hazard component using high-resolution numerical models, it is possible to identify receptors, their positions, and characteristics at the urban and suburban scales. The position of a receptor is critical to determining the magnitude of the hazard affecting it, and it represents the exposure. The characteristics and functionality of the receptor govern the possible impact of the hazard on the building (and/or its contents), thus representing its vulnerability. Floods have direct and indirect impacts on variable spatial and temporal scales (Rose, 2004; Viavattene et al., 2018; Armaroli et al., 2019). Direct impacts, associated with the physical interactions between flooding and assets, have local and instantaneous effects. In contrast, indirect impacts span from local to regional, and even to national and international scales; they can persist in the medium to long term, affecting, for example, flows of stocks and people at different levels through chain reactions. The latter are generally the most difficult to assess (see, for example, Meyer et al. (2013) for a review of applicable methods). Nonetheless, there exist various direct impacts that require evaluation; floods can damage buildings, contents, infrastructure, people, ecosystems, and so on. Generally, direct impacts are associated with hazard-induced property damage. Damage can be quantified using various methodologies, focusing on general damage or more specific damage (e.g. differentiating damage to contents from that to structures/buildings).

Uncertainties are generated throughout the risk assessment process and are propagated to the final results. Hazard modelling represents an important factor affecting the uncertainty of flood risk assessments (e.g. Vousdoukas et al., 2018a). However, proper representation of the consequences for the exposed receptors is also challenging, and is a dominant factor for the uncertainty of the entire assessment (de Moel and Aerts, 2011; Jongman et al., 2012; Figueiredo et al., 2018). Human assets show strong variability in space and time; therefore, vulnerability and exposure assessments are affected by uncertainty at various temporal and spatial scales (Figueiredo and Martina, 2016; Nguyen et al., 2016). Simplifications, as well as the characteristics of the chosen methodological approach, can increase the overall uncertainty of impact assessment. Uncertainties in flood damage evaluations can be categorised as aleatory and epistemic (Merz and Thieken, 2009). The former are related to the representativeness of the variables used for the assessment: for example, the buildings of a specific category are represented by a representative building that is assumed to portray all the characteristics of that specific group, disregarding any information on its variability. The latter are related to incomplete understanding of the analysed system and may be reduced by additional observations and research. Aleatory uncertainties are generally dominant for small flood events, while epistemic are dominant for larger ones (Wagenaar et al., 2016). Uncertainties can be partially reduced in both cases, but not removed. As demonstrated by the heterogeneity of the available studies showing, for example, various vulnerability functions for similar receptors, the quantification of impacts is strongly scale- and site-dependant (Figueiredo et al., 2018). Moreover, most studies have employed deterministic (i.e. single damage model-based) approaches (Gerl et al., 2016) — rarely with a proper discussion of limitations and uncertainty — or with detailed information on applicability constraints (e.g. applicability on different geomorphologic and socio-economic contexts than those where the models were developed). This last aspect, in particular, is very important when selecting a proper damage model (Wagenaar et al., 2016; Molinari et al., 2020).

Uncertainties related to flood risk assessments should be taken into account especially when communicating risk science to end-users (e.g. for this specific case, the coastal managers; Poljanšek et al., 2017), to avoid misinterpretation of the results that could lead to sub-optimal decisions and thus to the inappropriate allocation of resources (Wagenaar et al., 2016; Figueiredo et al., 2018). At the operational level, however, the (ab)use of non-probabilistic forecasts, often interpreted disregarding their limitations and uncertainty, can lead to mistrust of the forecasting system. It was demonstrated that properly informed decision making, generally based on integrating physical and social sciences through a participatory process, is very effective in preparing risk management plans and actions (Barquet and Cumiskey, 2018).

Methodologies capable of integrating and analysing results generated by diverse approaches and/or input parametrisations (e.g. probabilistic approaches, model ensembles; Dottori et al., 2016; Wagenaar et al., 2016; Figueiredo et al., 2018) represent valuable solutions to take uncertainties into account. It was demonstrated that the predictive skills of impact assessment approaches based on multiple damage models are higher than those of any single-model-based approach (Figueiredo et al., 2018). Indeed, although such methods probably lack precision from a deterministic perspective, they can provide a spectrum of possible results, including a component caused by the uncertainty of the entire assessment process. Thus, a properly trained end-user, whether a technician or a decision-maker, can consider both the most probable results and their uncertainties (which also include the almost-unrealistic-but-not-impossible occurrences).

This study reports the results of a numerical assessment of coastal flood direct impacts for the city of Stavanger (Rogaland, Norway). It was implemented in the framework of the European Union's Horizon 2020 (EU H2020) "EnhANcing emergencY management and response to extreme WeatHER and climate Events" project (ANYWHERE; www.anywhere-h2020.eu). The approach simulates historic extreme water level events (tide + non-tidal residuals) in the current situation and possible relative sea level rise (RSLR) scenarios by the end of the century, computing the hazard and direct impact components (i.e. damage to properties) at the receptor scale. The hazard assessment was implemented with a two-dimensional numerical model (LISFLOOD-FP) in a deterministic manner. Impacts were calculated considering multiple damage models. The results were analysed and shown semi-probabilistically, accounting for the uncertainty of the outcomes.

2. Methods and data

2.1. Approach overview

The flood impact assessment for the Stavanger municipality was based on the approach presented in Fig. 1. The hazard component was identified using a numerical model forced with historical events. The events were identified using data collected between 1988 and 2017 by the Stavanger tide gauge. They were simulated in the current and RSLR scenarios to analyse the possible evolution of impacts by the end of this century. The associated direct impacts were calculated based on the source–pathway–receptor–consequences concept (Floodsite, 2009; Narayan et al., 2014; Oumeraci et al., 2015; Sanuy et al., 2018), in the form of relative and financial damage at the receptor' scale, thus considering the exposure and vulnerability of each asset. Vulnerability was determined by the typology of the receptors (the categories considered in this study were residential, commerce, industry and transport). The evaluation quantified direct impacts on buildings, disregarding any information on their contents or on any possible direct impact on other properties (e.g. cars). Although the calculation of the hazard component was merely deterministic, because it was implemented through a single-parametrisation flood model forced with the observed time-series (i.e. total water levels) of historical extreme events, the consequences were calculated by applying several vulnerability curves (i.e. flood damage curves) for the selected typologies of the receptors. Financial

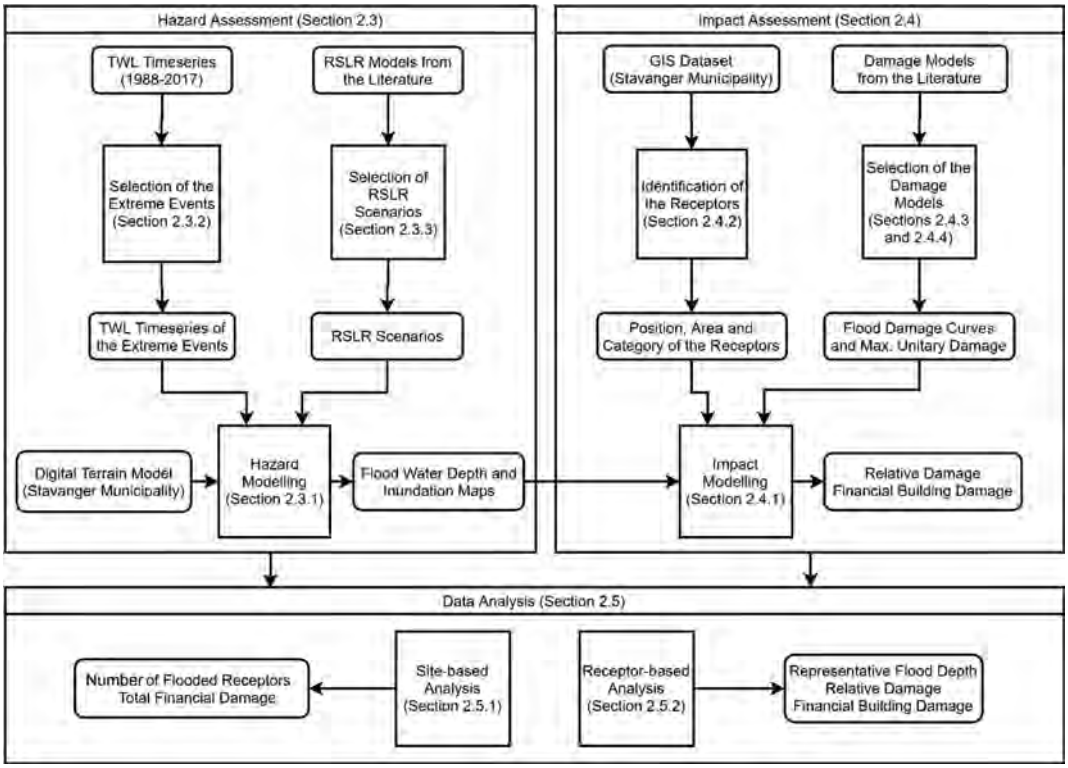

Fig. 1. Workflow of the approach used in this paper to assess coastal flood impact in Stavanger (Rogaland, Norway). The boxes refer to the sections of the paper.

damage was calculated when the flood-damage curve utilised is associated with the maximum unitary financial damage. The results were then analysed at the site and receptor scales. The case study location and characteristics are presented in Section 2.2. Details on the hazard assessment are provided in Section 2.3. The methodological approach to quantifying the impacts is described in Section 2.4. The site- and receptor-based analysis of the impacts is explained in Section 2.5.

2.2. Case study

Stavanger is the largest municipality in the Rogaland region of Norway (Fig. 2). Although it is an important industrial centre (Hatakenaka et al., 2011), it also represents an important tourist destination, as demonstrated by the many cruise ships that moor in its harbour every day, unloading thousands of tourists. The main attractions are the city cultural heritage sites, and nearby natural and historical sites. The city around the harbour recently underwent development in response to tourist demand. Commercial activities have thrived, and today the harbour area is occupied by many restaurants, pubs, hotels, and gift shops (see areas 1–4 in Fig. 2). In the framework of the ANYWHERE project, the municipality expressed its interest in knowing the possible impacts of extreme marine storms, also considering the possible changes induced by the ongoing climate crisis. Indeed, whereas the last very extreme event (maximum total water level of 1.17 m recorded at the Stavanger tide gauge), which happened in 1994, flooded a few properties in the north-eastern areas, and affected some commercial activities at the waterfront of the harbour (see Fig. 3A, B and C), the projected RSLR is likely to enhance future impacts, thus generating greater losses. As such, a recent exposure-based coastal flood impact assessment (Breili et al., 2019) shows that for a 20-year return period event, a 35% increase of exposed buildings is expected in Norway considering RSLR projections to 2090 based on the 95th percentile of Representative Concentration Pathway 8.5 (RCP8.5). This scenario corresponds to a RSLR of around 0.7–0.8 m at the Rogaland coast (Simpson et al., 2015, 2017; Breili et al., 2019). Locally, the increase of exposed elements may be higher. Stavanger was mentioned by Breili et al. (2019) as one of the locations that will become most vulnerable to coastal flooding. The flood damage assessment focuses on the areas highlighted in Fig. 2. The south-westernmost parts (1–4) represent the areas close to the harbour with high density of commercial activities. The other areas (5–9) mostly include residential buildings and some industrial activities.

2.3. Hazard assessment

2.3.1. Modelling approach

The potentially flooded area was evaluated with the LISFLOOD-FP (Bates and De Roo, 2000; Bates et al., 2005) flooding model, which can simulate the dynamic propagation of floods in different environments (e.g. fluvial, coastal, etc.). The computational domain (Fig. 4) covered an area of ~4.2 km^2 with a spatial resolution of 2 m. The topography was extracted from a 2014 Lidar-based digital terrain model (DTM; horizontal resolution: 0.2 m; datum: mean sea level 1996–2014, Stavanger tide gauge; www.kartverket.no) provided by the Stavanger municipality (Fig. 4). The flood model was forced with time-varying (time step: 10 min) water level conditions (measured tide + non-tidal residuals; see Section 2.3.2) imposed along the coastline boundary. Because of the small computational domain, the total water level was considered constant in space. The fixed time-step 2D solver version was applied. The infiltration coefficient was set to 1e-6, considering the characteristics of the urban area. The friction coefficient (i.e. Manning's *n* value) was set to 0.01, which represents the minimum value for trowel-finished concrete (Chow, 1959). The simulated outputs were stored with a time step of 30 min.

2.3.2. Selection of the extreme events

The total water level (TWL) data were retrieved from the Stavanger tide gauge (58.974339N 5.730121E). The time-series covered the period 1988–2017. First, an extreme value analysis based on the peak-over-threshold (POT) and the generalized pareto distribution (GPD)

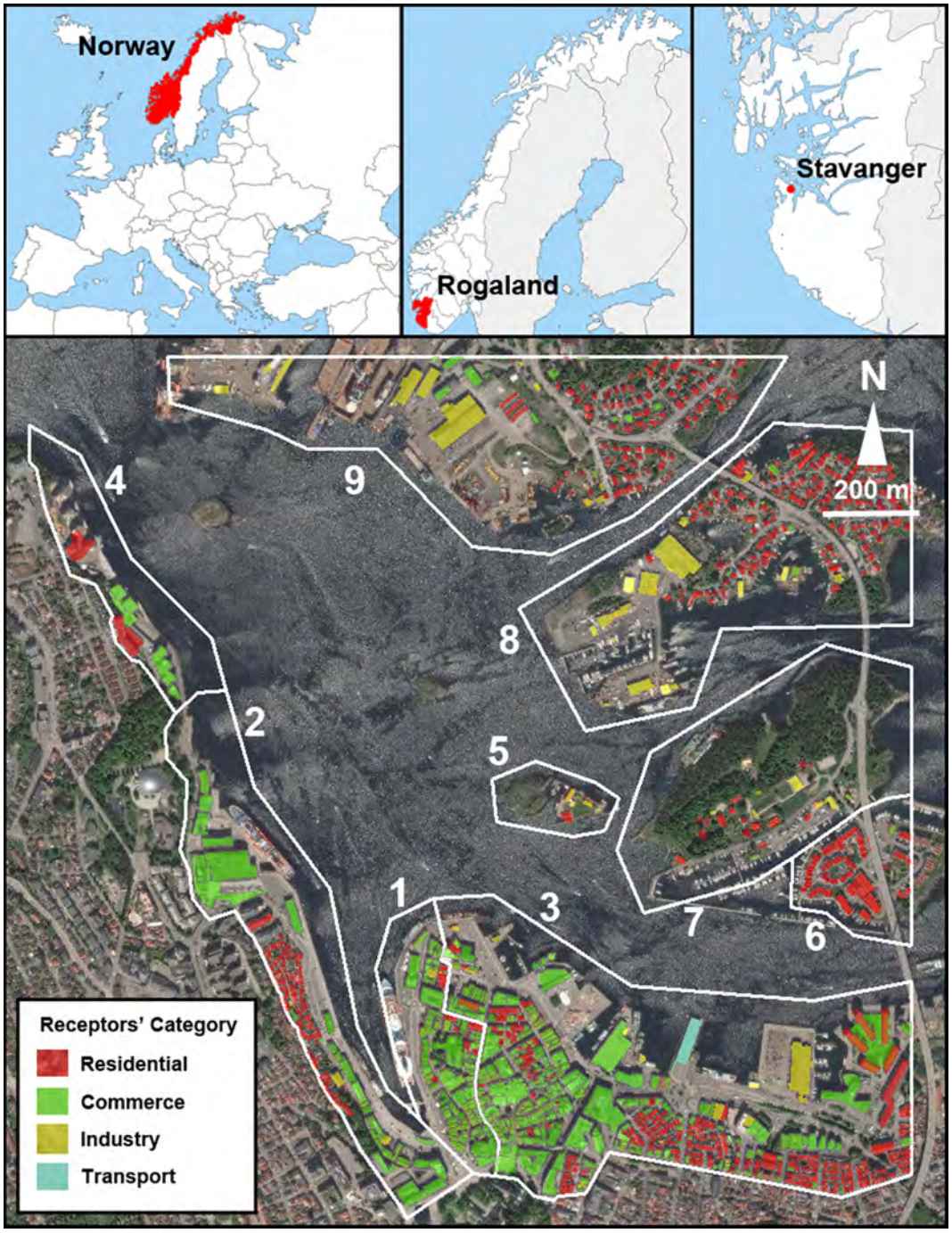

Fig. 2. Location of the study case. The Stavanger site was divided into smaller areas to simplify the analysis: (1) Stavanger harbour eastern waterfront; (2) Stavanger harbour western waterfront; (3) East Stavanger city centre; (4) Kalhammaren; (5) Plentingen and Natvigs Minde; (6) Grasholmen; (7) Sølyst; (8) Engøy; and (9) Buøy. The receptors considered are shown along with the categories they belong to—residential, commerce, industry and transport. (For interpretation of the references to colour in this figure legend, the reader is referred to the web version of this article.)

was applied to the TWL time-series (e.g. Vousdoukas et al., 2016). Threshold exceedance was identified when the water level measured at the tide gauge was higher than the threshold based on the 0.998 quantile of the whole time-series. Two exceedances were considered independent when separated by a time period longer than 72 h (i.e. meteorological independence criterion, MIC). This ensured an average of 4–5 exceedances per year. The POT values were used to fit a GPD.

The fitted GPD was then used to assess the 1-in-1 and 1-in-2 year TWL values. The 1-in-2 year value was set as the threshold to discard (i.e. values lower than the threshold) the "non-extreme" exceedances identified through the POT. Then, it was assumed that each "extreme" exceedance (i.e. values equal or higher than the threshold) identified the "peak" of the "extreme" event (storms). The start and end times of the storms were identified as the time values before and after the peak, respectively, when the TWL decreased below the 1-in-1 year threshold, and verified the independence criterion (in this case, half of the MIC). The identified time-series were then analysed to identify the maximum TWL, astronomical tide levels, and non-tidal residuals (i.e. measured TWL minus the astronomical tide). The astronomical tide was calculated using the Matlab code t_tide (Pawlowicz et al., 2002), based on a year-by-year analysis of the entire TWL time-series.

Fig. 3. (A, B and C) Flooded commercial activity areas in the Stavanger harbour during the extreme event that occurred in December 1994. The snapshots were retrieved from the YouTube video available at https://www.youtube.com/watch?v=vO66cd9A_b0 (last access: 13 January 2020). (D) Stavanger harbour during the flood which occurred on 30 January 2013. The picture was taken by Jostein Berggraf (Stavanger municipality) at 13:03 CET.

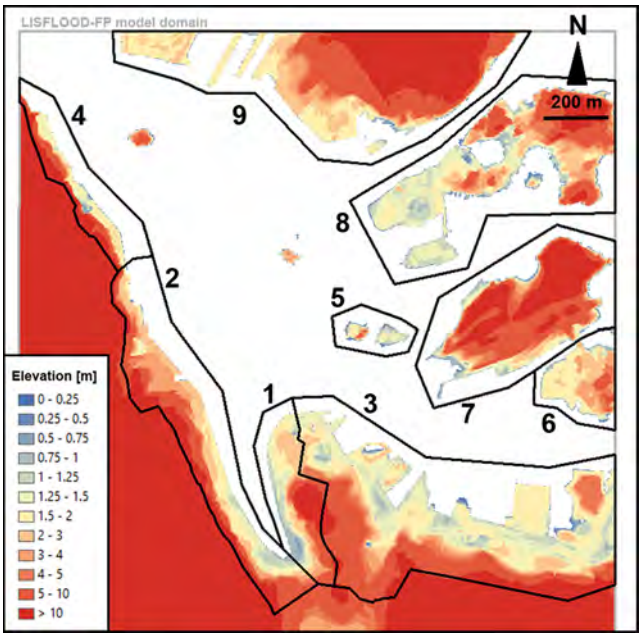

Fig. 4. Model domain and digital terrain model (datum: mean sea level 1996–2014, Stavanger tide gauge; www.kartverket.no) used for the hazard modelling with LISFLOOD-FP. Refer to Fig. 2 for the legend of the area numbers. (For interpretation of the references to colour in this figure legend, the reader is referred to the web version of this article.)

2.3.3. Selection of the relative sea level rise scenarios

Recent studies (Simpson et al., 2015, 2017; Breili et al., 2019) demonstrated that RSLR will increase the coastal flood hazard and risk in Norway, with important effects in Rogaland and, specifically, in Stavanger. Thus, any risk assessment should include the evaluation of future projected scenarios, especially at the local-scale. The RSLR scenarios were generated by increasing the level of the input TWL time-series at the model boundaries. The RSLR scenarios were based on results published by Simpson et al. (2012, 2015, and 2017; Table 1). Given the variability of the assessments, four RSLR scenarios were tested in this study: 0.32, 0.6, 0.9, and 1.21 m. The first value (0.32 m) was selected because it is comparable to the range of the TWL of the selected historical storms (0.28 m). The upper value (1.21 m) represents the highest of the assessed SRLR scenarios (Table 1). The other values (0.6 and 0.9 m) were selected as intermediate scenarios to support the analysis. The selected scenarios do not represent future projections (e.g. for a specific year and a specific emission scenario), but they are useful to analyse the sensitivity of the impacts to changes in relative sea level.

2.4. Impact assessment

2.4.1. Modelling approach

The impacts considered in the analysis referred only to direct impacts to assets. The impacts on exposed receptors (see Section 2.4.2) were assessed using flood-damage curves (FDCs) applied at the receptor scale (see Section 2.4.3), which represents a practical implementation of the unit loss method (De Bruijn, 2005; Wagenaar et al., 2016). An FDC describes the relation between the maximum flood water depth (*fwd*) affecting the receptor and the expected damage. It depends on the category of the receptor. The damage can be expressed in financial terms (e.g. as unitary damage, meaning the damage per unit of area of the asset, in €/m^2) or through a damage factor (a), from 0 to 1. When the damage factor is used, it can be applied to assess the unitary damage by multiplying it by the maximum unitary damage (UD_{max}), which depends on the category of the affected receptor, expressed in

Table 1
Relative sea level rise assessments for Stavanger considered to define the RSLR scenarios tested in this study.

Source	Base data	Projection	Range [m]		Emission scenario
			Min.	Max.	
Simpson et al. (2012)	1980–1999	2090–2099	0.02	0.58	IPCC AR4 SRES scenarios
			0.32	1.21	High-end scenario (upper bound)
Simpson et al. (2015) Simpson et al. (2017)	1986–2005	2081–2100	0.05	0.5	IPCC AR5 RCP2.6
			0.12	0.58	IPCC AR5 RCP4.5
			0.25	0.79	IPCC AR5 RCP8.5
		2100	0.04	0.54	IPCC AR5 RCP2.6
			0.12	0.63	IPCC AR5 RCP4.5
			0.28	0.9	IPCC AR5 RCP8.5

Europe in €/m^2. The expected damage (D) for a given flood water depth for a specific receptor is obtained by multiplying the unitary damage for the area (i.e. footprint) of the receptor.

For each receptor category, several FDCs can be found in the literature. Risk assessments are generally performed by applying one curve for each category (or land use category, for large-scale assessments; Gerl et al., 2016). Some studies have merged FDCs to obtain average curves for each category to provide more general damage models (e.g. the EU-scale FDCs provided by Huizinga et al., 2017). Risk assessments based on single damage models generate deterministic outcomes (Gerl et al., 2016; Figueiredo et al., 2018), and their uncertainty can be assessed through sensitivity analysis and/or by comparing the assessments with observed data (very often difficult to collect/obtain). Recently, damage assessments have been moving towards more (semi-)probabilistic approaches (Dottori et al., 2016; Figueiredo et al., 2018), enabling representation of the damage figure and its associated uncertainty.

In this study, for each category of receptors, all the available curves found in the literature were applied, after they were filtered to discard the less reliable ones (for more details, see Section 2.4.3). In practical terms, this means that for each receptor affected by the flooding caused by a single extreme event, more than one value of the damage factor was calculated, and multiple values of expected damage were thus obtained. When the maximum unitary damage was available, the expected financial damage was also calculated according to the procedure outlined in Section 2.4.4.

To generate a flood map for the generic simulated storm, the maximum *fwd* for each cell of the modelling domain was calculated. Then, the representative *fwd* was calculated for each mapped receptor (see Fig. 2). The representative *fwd* was defined as the average of the maximum *fwd* retrieved for each cell of the domain overlapping the receptor's footprint and a buffer of 2 m around it. A receptor was considered flooded when the representative *fwd* was higher than or equal to 0.05 m, to take into account the numerical uncertainty of the simulated water depth in relation with the uncertainty of the DEM, and background numerical noise. This threshold represents a reasonable compromise between the reliability of the *fwd* able to generate the damage, and the loss of information that a higher threshold would lead to. For each simulated event, the number of flooded receptors (N) was identified. For the generic receptor (n) affected by the representative flood water depth (fwd_n), the vector of the damage factors (a_n) was calculated as (Eq. (1)):

$$\alpha_n = [\alpha_{n,i}] = [\alpha_{n,1}, \cdots, \alpha_{n,k}] = [FDC_1(fwd_n), \cdots, FDC_k(fwd_n)] = [FDC_i(fwd_n)] \quad (1)$$

where k is the number of flood-damage curves (FDC_i with $i = 1, \ldots, k$) identified for that receptor category. Then, if the value of maximum unitary damage ($UD_{max,i}$) was available for the FDC_i, the expected building financial damage ($D_{n,i}$) was calculated as follows (Eq. (2)):

$$D_{n,i} = \alpha_{n,i} \cdot UD_{max,i} \cdot A_n \quad (2)$$

where A_n is the area (i.e. footprint) of the receptor n. The representative expected building financial damage for that receptor (D_n) was calculated as the average of the available $D_{n,i}$ (Eq. (3)):

$$D_n = mean(D_{n,i}) \quad (3)$$

The total assessed financial damage for the storm (D_{tot}) was calculated as the sum of the values of D_n, for each receptor exposed to flooding ($n = 1, \ldots, N$) (Eq. (4)):

$$D_{tot} = \sum_{n=1}^{N} D_n \quad (4)$$

In this study, the number of affected receptors (N) and the total damage (D_{tot}) were calculated for each historical storm, in the current situation and RSLR scenarios. These values represented global variables at the case study scale. For the analysis at the receptor scale, the hazard (i.e. *fwd*) and impacts in terms of damage factors (i.e. a) were considered for each receptor category. For further details on the integrated analysis of the results of the simulated scenarios, see Section 2.5. In the following sections, details on the receptors (Section 2.4.2), flood-damage curves (Section 2.4.3), and financial damage (Section 2.4.4) datasets are provided.

2.4.2. Identification of the receptors

The receptors shown in Fig. 2 were identified using the georeferenced dataset provided by the Stavanger municipality, updated in 2017. For each receptor, the dataset included the definition of the subcategory/type of building. The receptors were then grouped into main categories based on the definition by Huizinga et al. (2017). At the case study scale, only residential, commercial, industrial and transport buildings were identified using the available data. To avoid excessive background noise, only buildings with a footprint area equal or higher than 5 m^2 were considered. This threshold represents a reasonable compromise between the representativeness of the simulated damage, and the loss of information that a higher threshold would lead to. Table 2 shows the description of the categories, along with their distributions within the domain, as well as examples of the subcategories present in the areas shown in Fig. 2.

2.4.3. Flood-damage curves

FDCs were used to assess the direct impacts on exposed receptors. The majority of the curves considered residential, commercial, and industrial buildings (or land use). For some of the curves, detailed information describing the type of damage considered was provided. For example, some curves described the damage to buildings and their contents (e.g. furniture, electrical systems, etc.), such as the curves used by Huizinga et al. (2017), whereas others only considered the damage to the buildings. In most of the cases, this information was not explicit, although it was possible to infer the required information through analysis of the shapes of the curves; for example, FDCs that considered damage to furniture only showed a steeper initial increase (i.e. for low water depths) than curves that considered damage to buildings (see

Table 2
Description of the receptor categories following Huizinga et al. (2017), examples of the subcategories present in the area (Fig. 2), and categories' distributions within the domain.

Receptor building category	Description (from Huizinga et al., 2017)	Examples of subtypes, as described by the Stavanger municipality	Number of receptors in the domain (and percentage)
Residential	Residential buildings such as houses and apartments and their contents. Damage to assets in residential areas that are not residential buildings (i.e. in the public area and gardens) is not included.	Single/multi-storey/(semi-)detached houses; townhouses; boat houses; property garages and annexes; etc.	847 (64.5%)
Commerce	Commercial buildings and their contents such as offices, schools, hospitals, hotels, shops, etc. Damage to assets in commercial areas (i.e. in the public area and vehicles) is not included.	Offices; administrative, town halls; banks, post offices; shops; hotels; restaurants; museums; schools; hospitals; religious buildings; etc.	396 (30.1%)
Industry	Industrial buildings and their contents such as warehouses, distribution centres, factories, laboratories, etc. Damage to assets in industrial areas (i.e. in the public area and vehicles) is not included.	Factories; workshops; storehouses; etc.	70 (5.3%)
Transport	Transport facilities. Roads, railroads and infrastructure not included.	Expedition and terminal building	1 (0.1%)

examples from Deckers et al., 2010; Wagenaar et al., 2016). Curves that considered damage to both furniture and buildings showed an intermediate behaviour between the two types of curves described above.

The FDCs used in this study were selected from a larger group collected from the literature. Some of the curves found in the literature were discarded for various reasons. Curves that showed very different behaviour from the majority were also discarded, especially when detailed information on the represented damage was missing. Additionally, the curves could describe a specific case representative only of the area where they were developed. Other curves were discarded because their domains of application in terms of flood depth were too small compared with the majority of the curves, which covered water depths from 0 to 5–6 m. This was the case of the curves used by Scorzini and Frank (2017), which only included water depths lower than 1.5 m. It follows that the selected dataset of damage models was rather homogeneous, although it presented a certain variability for residential, commercial, industrial, and transport buildings. Because the applied methodology considered a group of curves, rather than a single damage model, this variability was considered in the analysis. It follows that the limitation caused by the heterogeneity of the damage models was minimized.

The selected damage curves are graphically shown in Fig. 5 and summarised in Table 3 for each receptor category, along with their references and the scoring based on Figueiredo et al. (2018), for which the calculation is based on a qualitative, expert-based approach to analyse the reliability of FDCs prior to their application (see discussion in Section 4.2). In particular, the scoring is based on expert judgement of the characteristics of the curves in relation to the chosen case study. Factors to be considered are the type of physical variables used, the details on the characterisation of the receptors, the similarity of the site where the model is to be applied compared with the site where the model was originally built, the correspondence between the analysed flood and the type of flood used to build the model, and, finally, the variable used to quantify the damage. Scores are given for each factor. A final general score is obtained for each curve by multiplication of the scores, and curves can be comparatively assessed. Higher general scores *a priori* identify more reliable curves.

2.4.4. Financial damage assessment

The financial damage assessment was implemented considering the maximum unitary damage expected for each building category (see Section 2.4.1). This type of information can be derived by analysing the construction/rebuilding costs of buildings at the national/international level or can be found in the literature, usually associated with an FDC. For this study, information collected in the literature was used. However, such data were retrieved for the curves (for Europe and Norway) provided by Huizinga et al. (2017) only. The same information was not available for the other models. The data are summarised in Table 4.

Given the few available data sets, the assessments of financial damage could not be interpreted in fully probabilistic terms (see Section 4.2). However, this method was still able to provide an indication of the total damage, especially when different scenarios were compared.

2.5. Data analysis

The large number of simulations produced results that were analysed considering two spatial scales. First, to give an idea of the simulated impacts that storms can generate at the case study scale (i.e. site-based analysis), the total number of impacted receptors and the estimated total mean damage were considered for each simulation. Then, impacts in the form of the damage factor and building financial damage were considered at the receptor scale (i.e. receptor-based analysis). In both cases, the results were presented using statistical descriptive variables (e.g. quantiles), histograms (relative frequencies), or ranges for given confidence intervals (e.g. 90/95%), generally built by considering the 5% and/or 95% quantiles of the (sub-)datasets. Thus, the results were provided in the form of distributions, and the outcomes were represented with indications of their uncertainty.

In some cases, the results were analysed by adopting different perspectives. First, impact results were shown as output generated by the dataset (or a constrained sub-dataset) of the forcing storm characteristics (i.e. input). Then, impacts were constrained (i.e. a range was selected). The corresponding distributions of forcing were analysed based on the assumption that they could represent the storm characteristics most likely to generate the selected range of impacts. The analysis/use of the results depends on the context. For emergency purposes, the most useful information is the relation between the input (e.g. a storm) and the associated outputs (e.g. damage). For prevention activities (e.g. land use planning), the perspective that relates the outputs (e.g. damage) to the input (e.g. forcing components) is of foremost importance.

2.5.1. Site-based analysis

A dataset was built considering all selected extreme events that were simulated in the current and RSLR scenarios, for a total of 80 records. For each of them, the total number of affected receptors (i.e. flood depth > 0.05 m; see Section 2.4.1) and the total financial damage were assessed. The results should be carefully considered, because the financial damage assessment was estimated based on very few available data (see Sections 2.4.1 and 2.4.4). Thus, the financial assessment for each storm should be considered as semi-deterministic. In addition, impacts were analysed by selecting groups of storms with similar characteristics. Thus, the results are presented in the form of distributions of possible impacts in terms of the number of affected receptors and total financial damage.

2.5.2. Receptor-based analysis

For the receptor-based analysis a dataset was built considering all simulated impacts at the receptor scale in the form of the damage factor and building damage, for all selected extreme events in the current situation and in RSLR scenarios. The entire dataset consisted of 111,968 records.

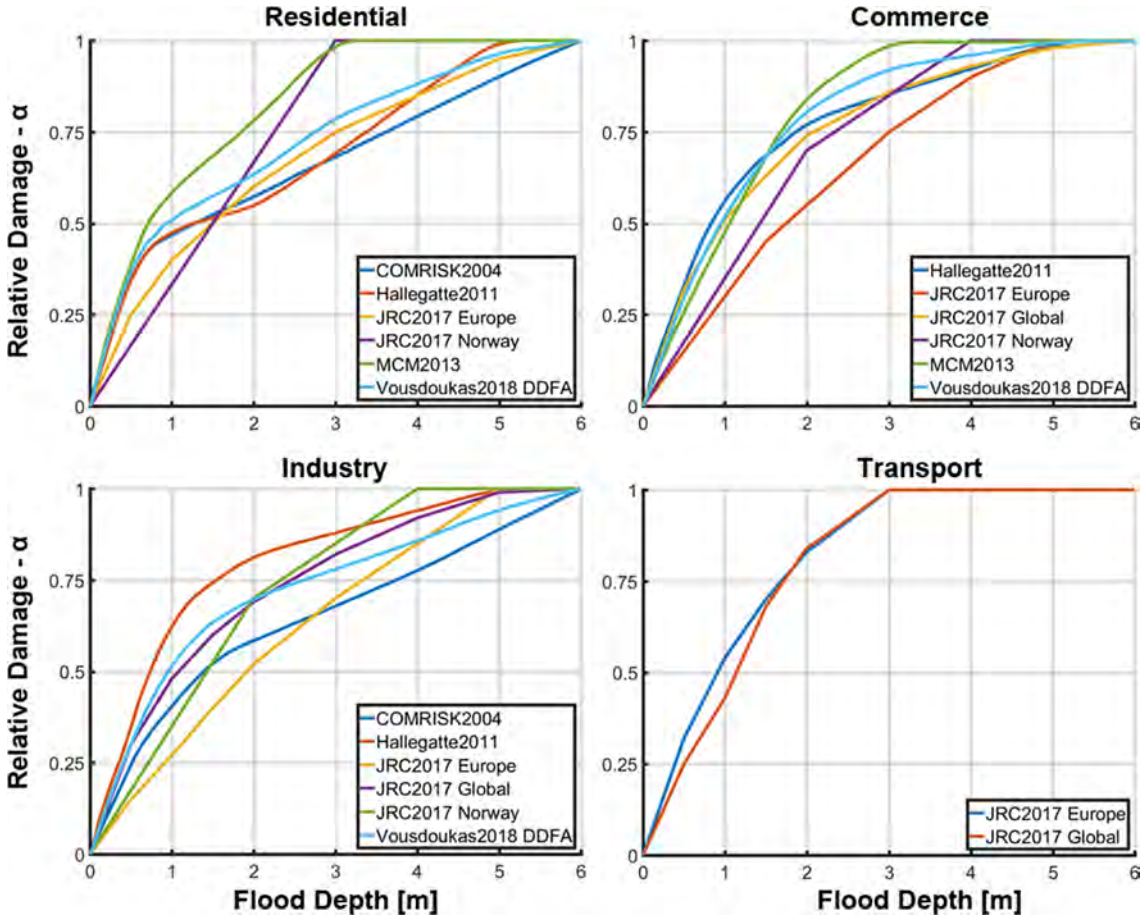

Fig. 5. Flood-damage curves for residential, commercial, industrial and transport building categories. Short names in the legends refer to Table 3. (For interpretation of the references to colour in this figure legend, the reader is referred to the web version of this article.)

For each flooded receptor (i.e. flood depth > 0.05 m) of each simulation, a set of damage factors was calculated using the representative flood water depth and all of the available damage curves, depending on the type of receptor. Thus, although the hazard was still assessed in a purely deterministic manner, the relative damage was calculated using a set of damage models. Therefore, the results include a quantification of the uncertainty of the impacts for each receptor. It should be noted that because the number of available flood-damage curves for each category differed, the dataset was homogenised using weights. Indeed, a residential, commercial, industrial receptor generated six values of relative damage, whereas a transport building generated only two values (see Fig. 5 and Table 3). To homogenise the representativeness within the dataset, a unitary weight was applied to the residential/commercial/industrial data, whereas transport data were weighted as three. Ranges of forcing were selected, providing the distribution of impacts. Additionally, ranges of impacts were selected for each receptor category (and/or all of them), providing the distribution of forcing that was most likely to generate the selected range of impacts for that receptor.

Table 3
Flood-damage curves adopted to calculate impacts to the identified receptors (R: residential; C: commerce; I: industry; T: transport). The scoring based on Figueiredo et al. (2018) is also shown (see Section 4.2).

Flood-damage curve			R	C	I	T	Damage model score based on Figueiredo et al. (2018)
Short name	Description	References					
COMRISK2004	Coastal FDCs for the Wadden Sea (estuarine environment)	Kystdirektoratet (2004) Vousdoukas et al. (2018a)	x	–	x	–	0.69e−2
Hallegatte2011	Coastal FDCs for Copenhagen	Hallegatte et al. (2011) Vousdoukas et al. (2018a)	x	x	x	–	0.69e−2
JRC2017 Global	Generic global FDCs	JRC report and database Huizinga et al. (2017)	–	x	x	x	0.29e−2
JRC2017 Europe	Generic FDCs for Europe	JRC report and database Huizinga et al. (2017)	x	x	x	x	0.29e−2
JRC2017 Norway	Generic FDCs for Norway	JRC report and database Huizinga et al. (2017)	x	x	x	–	0.44e−2
MCM2013	Coastal FDCs for typical UK properties. Adaptation of the fluvial depth-damage functions with an uplift factor to account for salinity.	Viavattene et al. (2015, 2018) Vousdoukas et al. (2018a)	x	x	–	–	0.69e−2
Vousdoukas2018 DDFA	Coastal FDCs based on small-scale coastal studies	Vousdoukas et al. (2018a)	x	x	x	–	0.69e−2
		Total	6	6	6	2	

Table 4
Maximum unitary damage from Huizinga et al. (2017).

Receptor building category	Maximum unitary damage from Huizinga et al. (2017)	
	Europe [€/m^2 − 2007]	Norway [€/m^2 − 2010]
Residential	750	729
Commerce	621	1,254
Industry	534	1,254
Transport	751	n/a

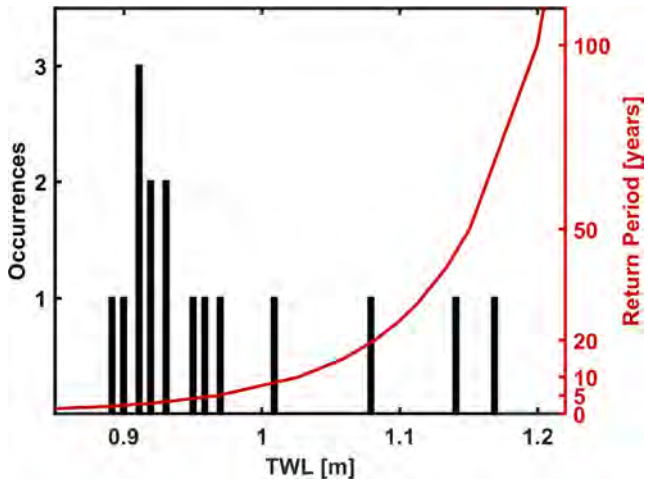

Fig. 6. Distribution of the maximum total water levels of the selected historical storms (in black) and assessed return periods based on the extreme value distribution analysis (in red). (For interpretation of the references to colour in this figure legend, the reader is referred to the web version of this article.)

3. Results

3.1. Selected extreme events

A total of 16 events were identified, distributed as shown in Fig. 6, along with indications of their return periods, which were assessed according to the procedure outlined in Section 2.3.2. Physical descriptions of the identified extreme events identified are shown in Table 5, where the maximum TWL (ranging from 0.89 to 1.17 m), astronomical tide levels, and non-tidal residuals are reported.

Table 6
Impacts at the case study scale: number of flooded receptors and estimated total damage by storm intensity in the current scenario. The results for all RSLR scenarios and all storms are included.

RSLR [m]	Group of storms	No. of flooded receptors			Estimated damage [Million € 2010]		
		Quantiles			Quantiles		
		5%	50%	95%	5%	50%	95%
0	TWL < 1.05 m	32	35	39	0.41	0.46	0.57
0	TWL > 1.05 m	44	45	50	0.71	0.8	0.87
0	All storms	32	35	49	0.41	0.46	0.85
All RSLR	All storms	33	112	290	0.44	2.4	11

3.2. Site-based analysis

The impacts analysed at the case study scale for the current scenario (RSLR = 0 m) are summarized in Table 6. Impacts presented low sensitivity to the intensity of the storm. Indeed, considering the low- (TWL < 0.95 m) and medium-intensity (TWL > 0.95 m and TWL < 1.05 m) storms and high-intensity storms (TWL > 1.05 m) in the current scenario, the flooded receptors and estimated (financial) damage did not show large variations, given the range of impacts in the whole dataset. The same low sensitivity to the TWL was seen in the other RSLR scenarios (data not reported here). However, the impacts of all storms consistently changed in magnitude with variation of the RSLR, as shown in Fig. 7. This result was expected as the extension of the range of the TWL of the simulated historical storms (0.89–1.17 m) is comparable with the TWL increment between the four simulated RSLR scenarios (~0.3 m). However, the behaviour of the relations between the RSLR and the impacts was not linear. It was indeed exponential-like, and the trend was emphasised for the estimated financial damage. The results show that the lower RSLR scenario (0.32 m) is likely to almost double the impacts expected for the current scenario. In the current scenario, 90% of the results showed less than 50 flooded receptors and estimated damage lower than €1 million (2010). To show this result from another perspective, the subset of simulations showing impacts with less than 50 flooded receptors and estimated damage

Table 5
Physical details of the selected historical storms. The recorded impacts (Norwegian Natural Perils Pool, 2019) regarding storm surge impacts for the Rogaland region are also shown.

ID	TWL Peak Date and Time	Duration [h]	Max. TWL [m]	Max. Tide* [m]	Max. Residual* [m]	Reported storm surge impact data in Rogaland (Norwegian Natural Perils Pool, 2019)	
						No. of damaged building	Total financial damage [NOK*1000]
1	15-Jan-1989 03:50	2.8	0.95	0.22	0.73	5	53
2	12-Feb-1990 00:00	1.5	0.89	0.31	0.59	–	–
3	27-Feb-1990 11:50	28.3	1.08	0.37	0.91	60	1,156
4	03-Jan-1991 12:10	2.8	0.97	0.40	0.59	–	–
5	20-Dec-1991 09:10	4.3	0.93	0.31	0.67	6	38
6	11-Jan-1993 12:10	39.2	1.14	0.35	0.84	63	966
7	08-Dec-1994 14:40	3.0	1.17	0.29	0.90	195	3,909
8	16-Jan-1999 21:40	2.3	0.93	0.26	0.68	–	–
9	30-Oct-2000 23:10	9.5	0.91	0.36	0.89	124	5,996
10	14-Dec-2000 00:10	14.2	0.90	0.41	0.61	–	–
11	12-Jan-2005 11:40	2.0	0.92	0.36	0.56	325	18,612
12	12-Jan-2007 16:20	4.8	1.01	0.17	0.85	17	547
13	30-Jan-2013 12:30	2.3	0.91	0.33	0.59	6	340
14	05-Dec-2013 11:40	1.0	0.91	0.44	0.48	19	574
15	10-Jan-2015 14:10	7.0	0.92	0.29	0.79	173	8,948
16	12-Jan-2017 10:20	2.7	0.96	0.34	0.65	13	319

* Can occur at different times than the Max TWL.

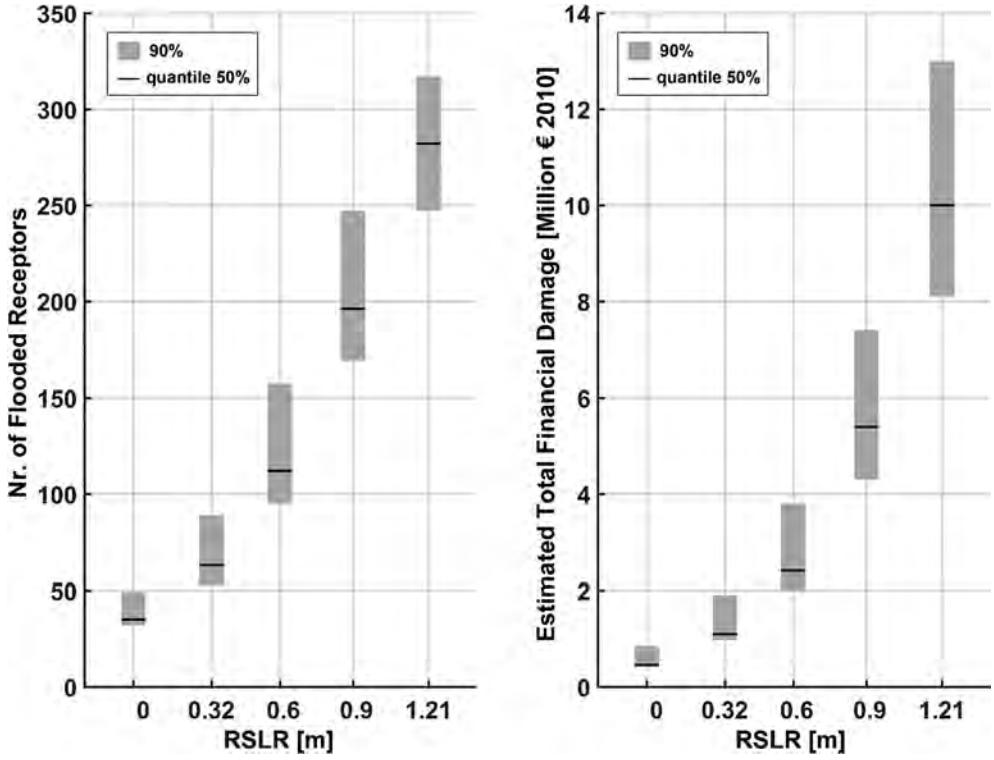

Fig. 7. Impacts at the case study scale: variations due to the RSLR scenarios of the number of flooded receptors and estimated total financial damage.

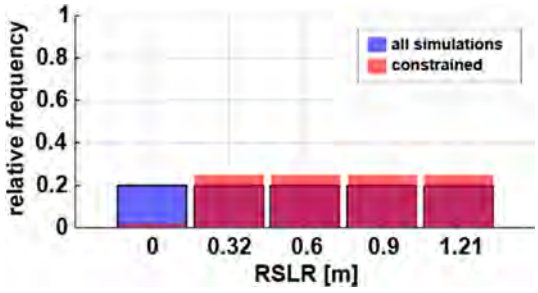

Fig. 8. Distribution of RSLR scenarios: in blue, the distribution of all simulations; in red, the distribution that is most likely to generate impacts with more than 50 flooded receptors and €1 million (2010) in damage. (For interpretation of the references to colour in this figure legend, the reader is referred to the web version of this article.)

higher than €1 million (2010) was extracted. The distributions of TWL and RSLR of the subset were analysed: the storm intensity distribution remained unvaried when compared with the whole dataset, but the RSLR distribution in Fig. 8 showed that such impacts are most probably expected for RSLR > 0 m.

3.3. Receptor-based analysis

The factors that combine to determine the distribution of the impacts to the receptors are multiple. The intensity of the forcing is the main factor, but the positions (i.e. areas in Fig. 2) of the receptors are also important. For the current scenario (RSLR = 0 m), the areas (see Fig. 2) that showed more calculated impacts were 8 (52.2%) and 9 (18.1%), possibly because of the high density of urbanisation and low elevations (see Fig. 4). In these areas, the most frequent impacts were calculated for residential buildings (>70%), the most abundant type of asset in areas 8 and 9 (see Fig. 2). Area 3 follows with 14.1% of calculated impacts. In area 3, most of the impacts were to commercial buildings (>40%), whereas impacts to residential properties were not present because of their locations in areas more elevated with respect to the mean sea level (see Fig. 4).

Residential buildings, which are present in all the areas shown in Fig. 2, were the most frequently affected receptors (~46% of the entire dataset). Nevertheless, the results showed that only those buildings located in areas 5 to 9 (north-east) were affected in the current and lowest (0.32 m) RSLR scenarios. For residential buildings, the impacts exhibited minor sensitivity to the intensity of the storm in the current scenario when compared with the entire dataset of residential impacts (Table 7). The higher quantile (95%) of (representative) flood depth

Table 7
Impacts at the receptor scale: (representative) flood depth, relative damage, and building financial damage of residential buildings grouped by storm intensity in the current scenario. The results for all RSLR scenarios and all storms are included.

RSLR [m]	Group of storms	Flood depth [m]			Relative damage			Building damage [x1000 € 2010]		
		Quantiles			Quantiles			Quantiles		
		5%	50%	95%	5%	50%	95%	5%	50%	95%
0	TWL < 1.05 m	0.06	0.12	0.32	0.03	0.08	0.22	0.6	2.6	11
0	TWL > 1.05 m	0.06	0.18	0.47	0.04	0.12	0.31	0.9	3.9	16
0	All storms	0.06	0.13	0.35	0.03	0.08	0.25	0.6	2.9	14
All RSLR	All storms	0.06	0.27	1.01	0.04	0.17	0.48	1.2	7.6	41

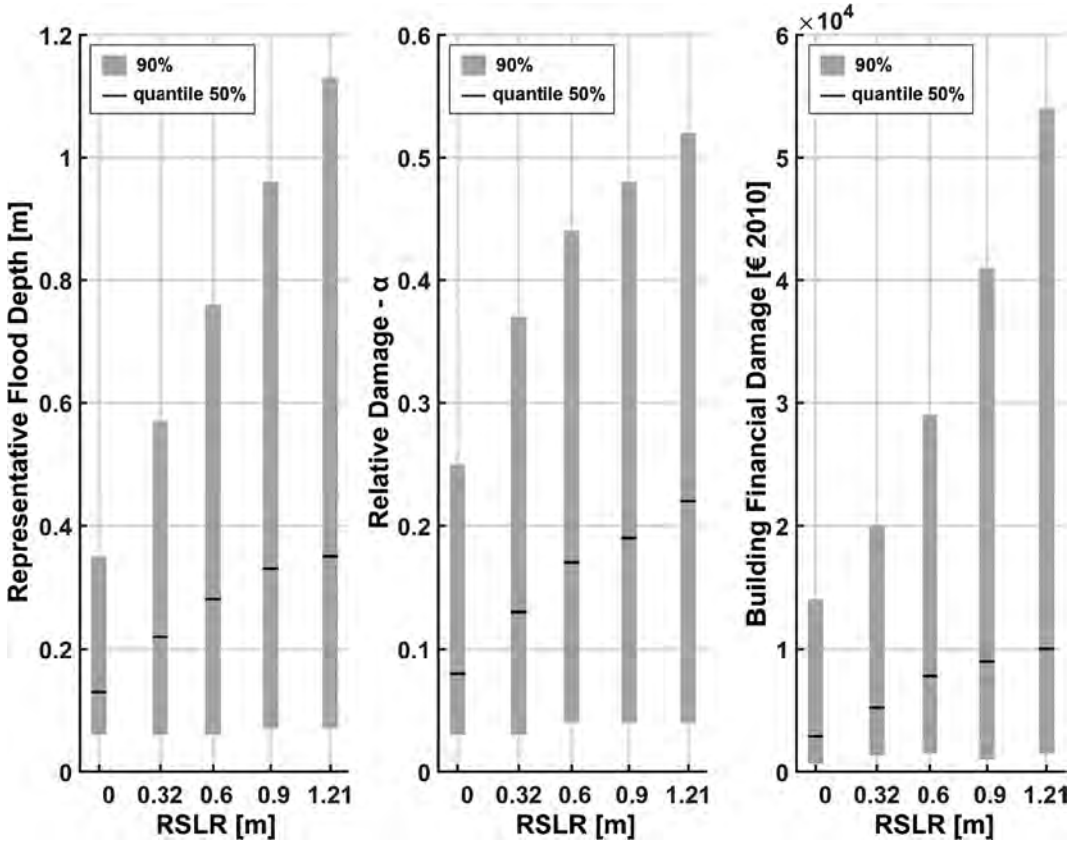

Fig. 9. Impacts at the receptor scale: variations associated with RSLR scenarios of (representative) flood depth, relative damage, and building financial damage to residential receptors.

expected for low- and medium-intensity storms (TWL < 1.05 m) and the high-intensity ones (TWL > 1.05 m) were around 0.32 and 0.47 m, respectively. The higher quantiles of relative damage and building financial damage also increased for high-intensity storms. Similar trends were observed for the other four RSLR scenarios (data not reported here). When the RSLR scenario was increased, the 50 and 95% quantiles of the distributions of flood depths, the relative damage and building financial damage also increased (Fig. 9).

The vulnerability of residential buildings to the forcing was analysed. Because the results showed minor sensitivity of the impacts to TWL, the main forcing was the RSLR scenario. The analysis of the vulnerability of residential buildings to RSLR is reported in Fig. 10. The dataset was constrained considering the sets of relative damage (α) to residential buildings with 95% confidence of being higher than 0.2, 0.3, 0.4, and 0.5. The graphs show that relative damage higher than 0.3 was not expected (or were negligible in frequency) for the current scenario, whereas relative damage higher than 0.5 occurred for RSLR ≥ 0.6 m. This was expected as it is strictly dependant on FDCs behaviour (see Fig. 5). Higher (representative) flood depths are expected for some buildings with increasing RSLR; therefore, higher relative damage is expected. Higher relative damage considered is associated with higher financial building damage (provided that the areas of the residential buildings are comparable), as shown by the distributions in Fig. 11. Thus, in general, the exponential-like behaviour of the estimated damage highlighted in the previous analysis (Fig. 7) is caused by both the increased number of affected receptors and the increased expected building financial damage.

4. Discussion

The impact analysis at the local scale is in line with most recent (semi-)probabilistic approaches proposed to calculate flood impacts (Wagenaar et al., 2016; Figueiredo et al., 2018). The study is comparable to ensemble-based studies (e.g. Figueiredo et al., 2018), as the

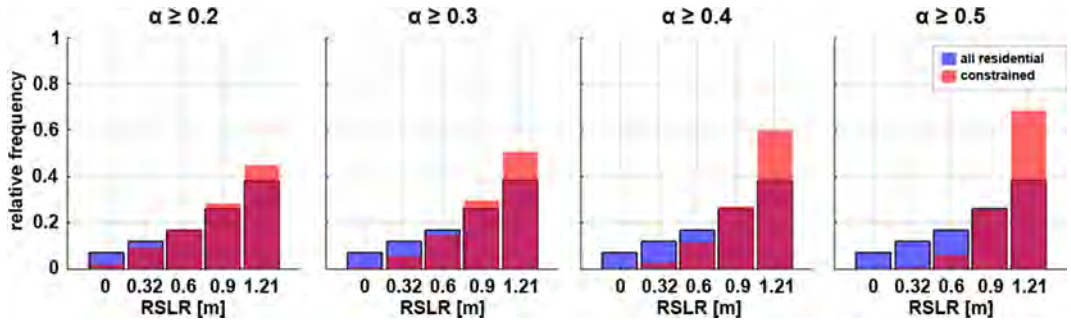

Fig. 10. Variation of the distribution of RSLR scenarios for relative damage to residential receptors with 95% confidence of being higher than 0.2, 0.3, 0.4, and 0.5. (For interpretation of the references to colour in this figure legend, the reader is referred to the web version of this article.)

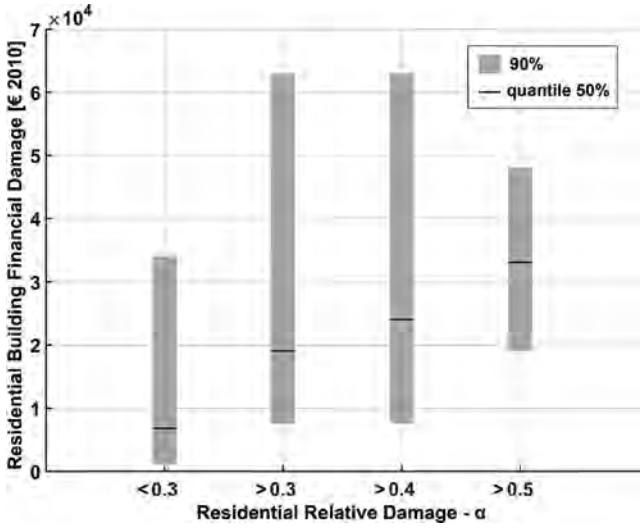

Fig. 11. Estimated building financial damage for relative damage to residential receptors with 95% confidence of being lower than 0.3 and higher than 0.3, 0.4, and 0.5.

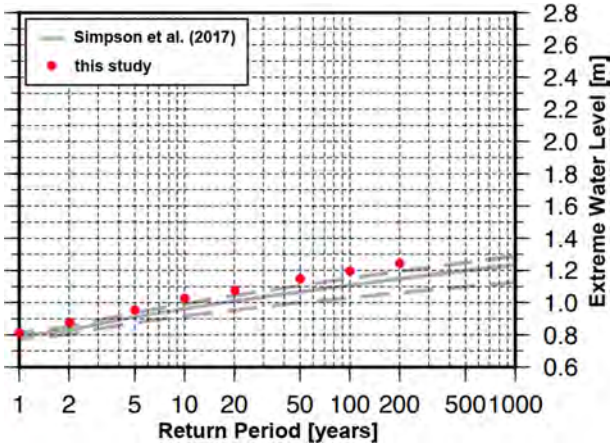

Fig. 12. Comparison between the outcomes of the extreme value analysis applied in this study (1988–2017; peak over threshold with generalized pareto distribution, in red) and that provided by Simpson et al. (2017) (1919–2014; average conditional exceedance rate; in grey, dashed lines represent the confidence interval), figure was adapted from Simpson et al. (2017). (For interpretation of the references to colour in this figure legend, the reader is referred to the web version of this article.)

dataset of impacts was generated using multiple damage models. Indeed, it represents a finite set of deterministic realisations of certain variables. However, the probabilistic interpretation of the outcomes of this study, meaning the presentation of the results as a distribution accounting for uncertainty, is frequentist (Weigel, 2011). This means that probabilities were estimated by taking the proportion of ensemble members (i.e. the dataset built with many simulations and receptor-based records) predicting the event. The analyses were performed considering groups of storms, rather than single-events separately. The results were not presented in deterministic terms, but rather shown as (un)constrained distributions generated by many (deterministic) data. This represents a very pragmatic approach. However, the reliability of the approach is dependent on the quality and number of the applied models. The reliability of the interpretation is higher if the number of ensemble models is large. The results were presented by applying quantiles (e.g. 5%, 50%, and 95%). This allowed the most representative outcomes to be shown, excluding outliers. Nevertheless, the choice of specific quantiles is not a clear-cut decision, as it depends on the person implementing the analysis. However, there was no need to extrapolate impact results out of the analysed domain of forcing (or vice versa) to pursue the aim of this work, and the representativeness of the outcome was ensured by coarse discretisation of the variables (e.g. grouping storms by intensity). Thus, applying a simple empirical cumulative distribution function to the data, or kernel functions to the ensemble models, was beyond of the scope of this work, even if a better representation and more reliable probabilistic interpretation could have been achieved (Weigel, 2011; Figueiredo et al., 2018).

The adopted approach allowed the results to be interpreted by considering an uncertainty range. In particular, this approach takes into account many sources of uncertainty (Merz and Thieken, 2009; Wagenaar et al., 2016), because it is based on the integration of three factors: (i) the modelling of hazard and impact components; (ii) the implementation of the analysis using (un)constrained variables (e.g. groups of storms), and (iii) the application of multiple damage models from different sources.

This study provides an interesting dataset of simulations of coastal flood direct impacts for the Stavanger municipality. In addition to the simplifications applied and the limitations of the approach discussed in Sections 4.1 and 4.2, it provides important input for administrators that may be interested in discussing local-scale coastal flood risk management plans with the support of quantitative information on possible current and future expected damages. The results are especially important to stimulate the discussion on the "do-nothing" scenario, which, according to the results of this study, may double the current impacts by the end of the century, considering only the most optimistic tested RSLR scenario (i.e. +32 cm). Note that the increased impacts are in line with the trends highlighted at the EU-scale by Vousdoukas et al. (2018b). At the Norway-scale, however, Breili et al. (2019) showed more optimistic trends on (potential) impacts, although they did not take into account the vulnerability of the exposed elements and did not perform local-scale analysis. Future works will focus on improving the hazard and impact modelling. The approach will be extended to other case studies, increasing the level of involvement of end-users to investigate its implications on policy and decision-making.

4.1. Hazard component

The historical storms were isolated after analysis of the water level data (see Section 2.3.2). The POT extreme value analysis was the preliminary step to isolate the storms. The outcomes of this analysis are compared in Fig. 12 with the results of Simpson et al. (2017), who determined the return period of extreme water levels for Stavanger using the "average conditional exceedance rate". The results of the present study tend to slightly overestimate the extreme water levels calculated by Simpson et al. (2017). The main reason could be the longer time-frame analysed by the authors (1919–2014). Additionally, as reported by the authors, the methodology applied by Simpson et al. (2017) to fit the extreme value distribution is more suitable for Norway, when compared with other approaches. However, the application of the extreme values calculated by Simpson et al. (2017) for storm isolation would have led to the identification of a larger number of minor storms. The difference is attributed to the 2-year return period value of TWL (which represents the threshold to filter non-extreme events) identified by Simpson et al. (2017), which shows a difference of ~10 cm with respect to the one calculated in this study. The duration of the storms would have remained almost identical, as the 1-year return period value (which represent the threshold for the identification of the start- and end-times of each identified storm) was comparable. In practical terms, the application of the method by Simpson et al. (2017) would have increased the representativeness of the dataset for (very) low intensity events, but it would have lowered the fraction of data related to medium- to high-intensity events.

In the absence of observed/measured flood maps of historical

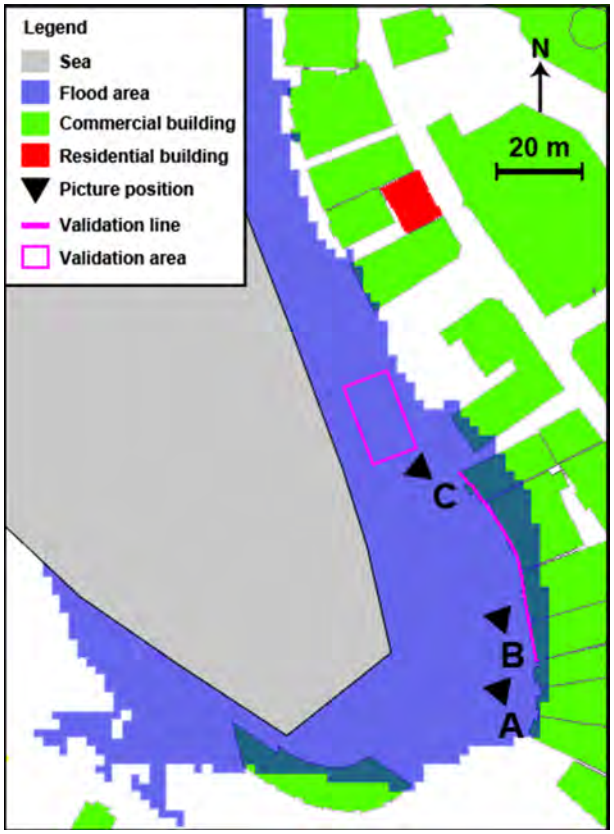

Fig. 13. Detail of the flood map of the December 1994 event (current scenario) for the Stavanger harbour area. The map includes the position where the snapshots in Fig. 3 were taken and the area where the validation of the flood depth was implemented. (For interpretation of the references to colour in this figure legend, the reader is referred to the web version of this article.)

events, the computed floodings were compared with publicly available pictures and videos (Fig. 3) to provide a semi-quantitative validation of the hazard assessment in the current scenario. A comparison between the model results and the flood that occurred during the extreme event of 8 December 1994 (TWL peak of 1.17 m) was carried out through comparison between the pictures in Fig. 3 (A, B and C) and the simulated flood map presented in Fig. 13. The positions where the pictures in Fig. 3 were taken were estimated and are shown in Fig. 13. The values of the simulated flood depths were extracted at the validation positions shown in Fig. 13 (purple line and rectangle), which roughly correspond to the building facades in Fig. 3A and B and the position where men are standing in Fig. 3C, respectively. The statistics of the flood depth assessment are shown in Table 8 and were compared with the visual estimation of the flood elevation at the same positions. The observed flood extent (Fig. 3) is qualitatively comparable with the simulated one (Fig. 13), and the values of flood depth are quantitatively comparable (Table 8). A similar qualitative comparison was implemented for an event that occurred on 30 January 2013 (TWL peak of 0.91 m). The picture in Fig. 3D was taken by Jostein Berggraf (Stavanger municipality) half an hour after the peak of the flood (Oda Roaldsdotter Ravndal, Kartverket – Norwegian Mapping Authority, personal communication). The picture shows the same area in Fig. 3, taken from a slightly different position. The comparison showed reasonable agreement with the simulated flood extent in the area (not reported here). Because the modelling approach is quite simplified and because no specific local phenomena are expected to affect the other areas of the case study, the hazard assessment can be considered reliable, at least in terms of the magnitude of the simulated flood extent and depths.

4.2. Impact component

In this study, the impact assessment focused on direct damage to property only. However, most of the considerations that follow may be applied and generalised to other types of direct impact assessment. Many impact studies (e.g. Apel et al., 2009; de Moel and Aerts, 2011) have concluded that flood hazard assessment does not represent a dominant factor for the whole assessment uncertainty, when compared with the uncertainty associated with damage assessment. A notable exception is Vousdoukas et al. (2018a), who pointed out that the input topographic dataset and hydrodynamic forcing can generate larger uncertainties in the impact assessment, when compared with those generated by damage models. However, the study was limited to few cases, and the conclusions were related to large-scale (regional) impact assessments. Thus, for local-scale studies, the uncertainty associated with the impact component remains a critical issue. This is indeed affected by large uncertainties (Jongman et al., 2012) that propagate to the final damage estimations, especially when damage calculations are applied deterministically (Figueiredo et al., 2018). The damage-to-building assessment was flawed because of the assumption that the damage is a function of the hazard and the building category. Improved assessment should be achieved by including more detailed (e.g. from cadastral to building-scale) information, and considering the subtype of building (e.g. single-storey or multi-storey), the socio-economic figure of the study area, and the degree of maintenance (see e.g. Dottori et al., 2016). Most FDCs were built without considering these variations. However, some studies have provided specific curves depending on the sub-type of building (e.g. Scorzini and Frank, 2017). Nonetheless, these FDCs are strongly site-dependant, and transferring them to other locations is more likely to produce larger uncertainty than using more general curves (Figueiredo et al., 2018). In addition to these aspects, more detailed phenomena were excluded from the analysis. In fact, the presence of basements was excluded, as well as the elevation of doors from the ground, although both are key contributors to flood damage. To include these aspects, extremely detailed data are necessary at the building scale (i.e. micro-scale). The type of flood hazard and related damage models are also important as marine floods are different from fluvial floods in terms of consequences to buildings (e.g. the effect of salt water on properties).

A way to properly select FDCs for impact assessment, even when probabilistic or ensemble approaches were used, was suggested in recent studies (e.g. Figueiredo et al., 2018). Figueiredo et al. (2018) provided a qualitative, expert-based approach to analyse the reliability of FDCs prior to their application (see Section 2.4.3). This approach was applied to the FDCs used in this study (Table 3), although the general scores were not considered for the selection of the curves. The scores

Table 8
Validation of the flood depths for the location shown in Fig. 13.

Position	Description	Visual estimation of flood depth in Fig. 3 [m]	Simulated flood depth [m]		
			Average	Standard deviation	Range
Line	Corresponds to the building facades in Fig. 3A and B	~0.15–0.2	0.19	0.03	0.14–0.25
Area	Corresponds to the position where men in Fig. 3C are standing	~0.2–0.25	0.23	0.03	0.16–0.32

demonstrate how curves specifically built for coastal flooding are *a priori* more reliable than the curves derived from fluvial studies. It is clear how the lack of site-specific curves may undermine the results. However, it was demonstrated that the use of multi-model approaches for damage assessment increases the predictive skills of losses (Figueiredo et al., 2018), compared with any single-model assessment.

The assessment of financial damage (and its uncertainty) is not as robust as the relative damage estimation. Indeed, although the relative damage was calculated using many flood-damage curves, the financial damage was based on a few maximum damage data. The choice to use the financial data associated with the curve for which the information was available was determined based on the importance of avoiding mix up maximum damage values associated with a specific function and FDCs from different sources (Wagenaar et al., 2016).

Damage assessments for future scenarios should include considerations of the possible evolution of receptors in terms of exposure and vulnerability. This is an important limitation that could be overcome by considering various scenarios of socio-economic growth (e.g. Vousdoukas et al., 2018b). It should be considered that, for coasts that have experienced economic and population growth in the last few years, it is very likely that in the future, the density of the receptors will increase. However, it could even decrease, depending on the evolution of socio-economic conditions. In addition, the type (and consequently the vulnerability) and economic value of the receptors may vary. The damage calculated for the current situation is not directly comparable with the damage calculated for the next decades and should be homogenised. However, to include such information, models of urban growth should be run together with socio-economic models able to project the expected modifications in terms of population growth and economic development. Such data are difficult to obtain and incorporate in an impact assessment of long-term scenarios. Furthermore, such a comprehensive analysis is beyond the scope of the present paper.

Validation of the impact component of the assessment was carried out by comparing the simulated distribution of residential building damage in the current scenario with impact data retrieved from the dataset of the Norwegian Natural Perils Pool (NNPP, 2019). The dataset includes daily information on the number of buildings that reported damage and the total amount of damage for each hazard. The data were integrated at the regional (Rogaland) level and refer to owners that insured their property with companies belonging to the NNPP. It follows that the dataset is partially incomplete and does not fully represent the real picture. For this reason, impact data was not used in absolute terms but rather manipulated and compared with the damage for residential buildings. The integrated data for Rogaland (Table 5) on the number of impacted receptors and financial damage (in nominal NOK) were retrieved for each historical event, considering a time frame that included the day(s) of each event and the following day (to take into account the fact that the records are stored with the date the damage was reported to the insurance company). The data in Table 5 were used to calculate the average financial damage to buildings for each event, to be compared with the distribution of building financial damage (Fig. 14). The nominal financial damage in NOK was converted into euros, considering the following average exchange rates (European Central Bank, 2019): 8.13 NOK/€ for the period 1999–2010 (range 7.22–9.95 NOK/€); 8.57 NOK/€ for the period 2010–2019 (range 7.27–10 NOK/€). The nominal damage values were then converted into real values considering the following Gross Domestic Product (GDP) deflator (Organization for Economic Co-operation and Development, 2019; available for the period 1996–2019): 80 in 1996, 100 in 2010 and 110 in 2019. Note that for damage recorded before 1996, the correction was applied considering the trend of 1996–2010. The comparison in Fig. 14 shows that the simulated distributions were comparable with the observed data, even if it is possible to notice a tendency to the under-estimation of the building damage for low-intensity events (TWL $<$ 0.95 m), and an over-estimation of the financial damage for high-intensity storms (TWL $\geq$ 1.05 m). Some low-intensity events

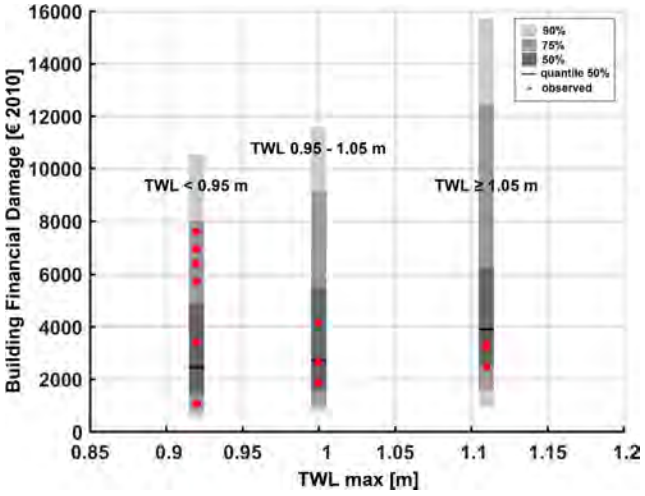

Fig. 14. Comparison between the distributions of simulated and observed building financial damage in € (2010) (Norwegian Natural Perils Pool, 2019). The comparison was carried out for the current scenario and residential buildings only. (For interpretation of the references to colour in this figure legend, the reader is referred to the web version of this article.)

showed observed (average) building damage higher than that of more intense events, as well as a higher variability. Indeed, for low-intensity events generating small flood events, the aleatory component of uncertainty (Merz and Thieken, 2009) was dominant. The few affected houses could show high variability in impacts that might not be properly represented by "average" models, which may, in contrast, work better for larger floods affecting a large number of receptors (Wagenaar et al., 2016). The distributions of simulated financial damage reflect this variability. Note that with increased storm intensity, the uncertainty increases. This reflects the fact that more intense events the epistemic component is larger and dominant (Wagenaar et al., 2016). This means that this approach is able to account for both aleatory and epistemic components of uncertainty. A similar comparison for other building categories was not possible because of the lack of data.

5. Conclusions

This work presents a coastal risk assessment application at the Stavanger municipality (Norway) based on recent advancements in impact evaluation. The impact assessment approach was carried out by combining numerical assessment of the hazard component (flood extent and depth; LISFLOOD-FP model, Bates and De Roo, 2000; Bates et al., 2005) with a damage assessment based on multiple damage models. The total water level time-series collected at the Stavanger tide gauge between 1988 and 2017 was analysed. An extreme value analysis based on peak-over-threshold (POT) and generalized pareto distribution (GPD) was applied to the TWL time-series (e.g. Vousdoukas et al., 2016) to identify extreme events to be used in the analysis in the current and RSLR scenarios. The RSLR data were extracted from previous works by Simpson et al. (2012, 2015, and 2017). The distribution of impacts was shown and discussed in the current and sea level rise scenarios. The analyses were presented at the scale of the case study, focusing on direct impacts generated by storms (i.e. the number of flooded receptors and total damage), and at the receptor-scale (built environment only), focusing on the damage that can be expected for building-type assets, given specific storm conditions and, conversely, by analysing the forcing components to which the receptors are most vulnerable. This approach is able to take into account many sources of uncertainty (e.g. Wagenaar et al., 2016) and represents a solution to provide an evaluation of damage at the local level, along with quantification of the uncertainty and reliability of the outcome. A quali-quantitative validation of the hazard modelling and financial damage estimation in the

current scenario was presented, demonstrating the reliability of the applied methodologies.

This analysis showed that the impact magnitude was more sensitive to the increase in relative sea level, rather than to the characteristics of the extreme event in the current scenario. The results showed that the expected impacts are fewer than 50 flooded receptors and less than €1 million in the current scenario. Impacts may double by the end of the century, considering the most optimistic increase of relative sea level. This quantitative local-scale assessment is of foremost importance to understanding the magnitude of possible current and future impacts, and can be used to implement cost-benefit analysis of local-scale mitigation and adaptation plans, to support the identification of optimal strategies. The limitations and simplifications applied were discussed to point out the aspects that should be taken into account for future improvements (of both hazard and impact evaluation). End-users should be deeply involved to investigate the implications of this approach on policy and decision-making, through a bottom-up approach.

CRediT authorship contribution statement

Enrico Duo: Conceptualization, Methodology, Software, Formal analysis, Investigation, Data curation, Visualization, Writing - original draft, Writing - review & editing. **Tomas Fernández-Montblanc:** Conceptualization, Methodology, Software, Investigation, Writing - review & editing. **Clara Armaroli:** Conceptualization, Writing - review & editing, Supervision.

Declaration of Competing Interest

The authors declare that they have no known competing financial interests or personal relationships that could have appeared to influence the work reported in this paper.

Acknowledgements

The authors are grateful to: Hugo Kind and Eirik Mannsåker (Stavanger Kommune), who provided most of the data needed for the analysis; Jan Sigurd Moy (Stavanger University Hospital), Jan Håvard Skjetne (Sintef), Valentina De Santis, and Oda Roaldsdotter Ravndal (Kartverket - Norwegian Mapping Authority) for their help in collecting and sharing information on the site; Marc Sanuy Vazquez (Universitat Politècnica de Catalunya) for his suggestions on data analysis; and Prof. Paolo Ciavola (University of Ferrara) for his precious contribution revising this work.

Funding

This work was supported by the EU H2020 ANYWHERE project (EnhANcing emergencY management and response to extreme WeatHER and climate Events; GA 700099; www.anywhere-h2020.eu).

References

[dataset] European Central Bank, 2019. ECB euro reference exchange rate. https://www.ecb.europa.eu/stats/policy_and_exchange_rates/euro_reference_exchange_rates/html/eurofxref-graph-nok.en.html (last access: 12 July 2019).

[dataset] Norwegian Natural Perils Pool, 2019. Natural Disaster Statistics. https://www.naturskade.no/statistikk/ (last access: 12 July 2019).

[dataset] Organization for Economic Co-operation and Development, 2019. "Main Economic Indicators - complete database", Main Economic Indicators. https://doi.org/10.1787/data-00052-en (last access: 12 July 2019).

Apel, H., Aronica, G.T., Kreibich, H., Thieken, A.H., 2009. Flood risk analyses—how detailed do we need to be? Nat. Hazards 49, 79–98. https://doi.org/10.1007/s11069-008-9277-8.

Armaroli, C., Duo, E., 2018. Validation of the coastal storm risk assessment framework along the emilia-romagna coast. Coast. Eng. 134, 159–167. https://doi.org/10.1016/j.coastaleng.2017.08.014.

Armaroli, C., Duo, E., Viavattene, C., 2019. From hazard to consequences: evaluation of direct and indirect impacts of flooding along the emilia-romagna coastline, Italy. Front. Earth Sci. 7, 203. https://doi.org/10.3389/feart.2019.00203.

Barquet, K., Cumiskey, L., 2018. Using participatory Multi-Criteria Assessments for assessing disaster risk reduction measures. Coast. Eng. 134, 93–102. https://doi.org/10.1016/j.coastaleng.2017.08.006.

Bates, P., De Roo, A.P., 2000. A simple raster-based model for flood inundation simulation. J. Hydrol. 236, 54–77. https://doi.org/10.1016/S0022-1694(00)00278-X.

Bates, P.D., Dawson, R.J., Hall, J.W., Horritt, M.S., Nicholls, R.J., Wicks, J., Ali Mohamed Hassan, M.A., 2005. Simplified two-dimensional numerical modelling of coastal flooding and example applications. Coast. Eng. 52(9), 793–810. https://doi.org/10.1016/j.coastaleng.2005.06.001.

Breili, K., Simpson, M.J.R., Klokkervold, E., Roaldsdotter Ravndal, O., 2019. High accuracy coastal flood mapping for Norway using LiDAR data. Nat. Hazards Earth Syst. Sci. Discuss. https://doi.org/10.5194/nhess-2019-217, in review.

Chow, V., 1959. Open-channel hydraulics. McGraw-Hill Book Co., New York.

De Bruijn, K.M., 2005. Resilience and flood risk management: A system approach applied to lowland rivers. PhD Thesis –. Delft University of Technology-, Delft, the Netherlands.

Deckers, P., Kellens, W., Reyns, J., Vanneuville, W., De Maeyer, P., 2010. A GIS for flood risk management in Flanders. In: Showalter, P.S., Lu, Y. (Eds.), Geospatial Techniques in Urban Hazard and Disaster Analysis. Springer-Verlag, pp. 51–69.

de Moel, H., Aerts, J.C.J.H., 2011. Effect of uncertainty in land use, damage models and inundation depth on flood damage estimates. Nat. Hazards 58 (1), 407–425. https://doi.org/10.1007/s11069-010-9675-6.

Dottori, F., Figueiredo, R., Martina, M.L.V., Molinari, D., Scorzini, A.R., 2016. INSYDE: a synthetic, probabilistic flood damage model based on explicit cost analysis. Nat. Hazards Earth Syst. Sci. 16, 2577–2591. https://doi.org/10.5194/nhess-16-2577-2016.

Dottori, F., Kalas, M., Salamon, P., Bianchi, A., Alfieri, L., Feyen, L., 2017. An operational procedure for rapid flood risk assessment in Europe. Nat. Hazards Earth Syst. Sci. 17, 1111–1126. https://doi.org/10.5194/nhess-17-1111-2017.

Figueiredo, R., Martina, M., 2016. Using open building data in the development of exposure data sets for catastrophe risk modelling. Nat. Hazards Earth Syst. Sci. 16 (2), 417–429. https://doi.org/10.5194/nhess-16-417-2016.

Figueiredo, R., Schröter, K., Weiss-Motz, A., Martina, M.L.V., Kreibich, H., 2018. Multi-model ensembles for assessment of flood losses and associated uncertainty. Nat. Hazards Earth Syst. Sci. 18, 1297–1314. https://doi.org/10.5194/nhess-18-1297-2018.

FLOODsite, 2009. Language of risk: Project Definitions. edited by: Samuels, P. and Gouldby, B. Wallingford, Oxfordshire, UK. available at: http://floodsite.net/html/partner_area/project_docs/T32_04_01_FLOODsite_Language_of_Risk_D32_2_v5_2_P1.pdf (last access: 11 July 2019).

Gerl, T., Kreibich, H., Franco, G., Marechal, D., Schröter, K., 2016. A Review of Flood Loss Models as Basis for Harmonization and Benchmarking. PLoS ONE 11 (7), e0159791. https://doi.org/10.1371/journal.pone.0159791.

Hallegatte, S., Ranger, N., Mestre, O., Dumas, P., Corfee-Morlot, J., Herweijer, C., Wood, R.M., 2011. Assessing climate change impacts, sea level rise and storm surge risk in port cities: a case study on Copenhagen. Climatic Change. 104, 113–137. https://doi.org/10.1007/s10584-010-9978-3.

Harley, M.D., Valentini, A., Armaroli, C., Perini, L., Calabrese, L., Ciavola, P., 2016. Can an early-warning system help minimize the impacts of coastal storms? A case study of the 2012 Halloween storm, northern Italy. Nat. Hazards Earth Syst. Sci. 16 (1), 209–222. https://doi.org/10.5194/nhess-16-209-2016.

Hatakenaka, S., Westnes, P., Gjelsvik, M., Lester, R., 2011. The regional dynamics of innovation: a comparative study of oil and gas industry development in Stavanger and Aberdeen. Int. J. Innov. Regional Develop. 3 (3–4), 305–323. https://doi.org/10.1504/IJIRD.2011.040528.

Huizinga, J., Moel, H. de, Szewczyk, W., 2017. Global flood depth-damage functions. Methodology and the database with guidelines. EUR 28552 EN. doi: 10.2760/16510.

Jongman, B., Kreibich, H., Apel, H., Barredo, J.I., Bates, P.D., Feyen, L., Gericke, A., Neal, J., Aerts, J.C.J.H., Ward, P.J., 2012. Comparative flood damage model assessment: towards a European approach. Nat. Hazards Earth Syst. Sci. 12, 3733–3752. https://doi.org/10.5194/nhess-12-3733-2012.

Kystdirektoratet, 2004. COMRISK SP7 Report – Risk Assessment of the Wadden Sea.

Merz, B., Thieken, A.H., 2009. Flood risk curves and uncertainty bounds. Nat. Hazards 51, 437. https://doi.org/10.1007/s11069-009-9452-6.

Meyer, V., Becker, N., Markantonis, V., Schwarze, R., van den Bergh, J.C.J.M., Bouwer, L.M., Bubeck, P., Ciavola, P., Genovese, E., Green, C., Hallegatte, S., Kreibich, H., Lequeux, Q., Logar, I., Papyrakis, E., Pfurtscheller, C., Poussin, J., Przyluski, V., Thieken, A.H., Viavattene, C., 2013. Review article: Assessing the costs of natural hazards – state of the art and knowledge gaps. Nat. Hazards Earth Syst. Sci. 13, 1351–1373. https://doi.org/10.5194/nhess-13-1351-2013.

Molinari, D., Ballio, F., Menoni, S., 2013. Modelling the benefits of flood emergency management measures in reducing damages: a case study on Sondrio. Italy. Nat. Hazards Earth Syst. Sci. 13, 1913–1927. https://doi.org/10.5194/nhess-13-1913-2013.

Molinari, D., Scorzini, A.R., Arrighi, C., Carisi, F., Castelli, F., Domeneghetti, A., Gallazzi, A., Galliani, M., Grelot, F., Kellermann, P., Kreibich, H., Mohor, G.S., Mosimann, M., Natho, S., Richert, C., Schroeter, K., Thieken, A.H., Zischg, A.P., Ballio, F., 2020. Are flood damage models converging to reality? Lessons learnt from a blind test. Nat. Hazards Earth Syst. Sci. Discuss. (in review). https://doi.org/10.5194/nhess-2020-40.

Narayan, S., Nicholls, R.J., Clarke, D., Hanson, S., Reeve, D., Horrillo-Caraballo, J., le Cozannet, G., Hissel, F., Kowalska, B., Parda, R., Willems, P., Ohle, N., Zanuttigh, B., Losada, I., Ge, J., Trifonova, E., Penning-Rowsell, E., Vanderlinden, J.P., 2014. The SPR systems model as a conceptual foundation for rapid integrated risk appraisals: Lessons from Europe. Coast. Eng. 87, 15–31. https://doi.org/10.1016/j.coastaleng.

2013.10.021.
Nguyen, T.T.X., Bonetti, J., Rogers, K., Woodroffe, C.D., 2016. Indicator-based assessment of climate-change impacts on coasts: A review of concepts, methodological approaches and vulnerability indices. Ocean Coast. Manag. 123, 18–43. https://doi.org/10.1016/j.ocecoaman.2015.11.022.
Oumeraci, H., Kortenhaus, A., Burzel, A., Naulin, M., Dassanayake, D.R., Jensen, J., Wahl, T., Mudersbach, C., Gönnert, G., Gerkensmeier, B., Fröhle, P., Ujeyl, G., 2015. XtremRisK – integrated flood risk analysis for extreme storm surges at open coasts and in estuaries: methodology, key results and lessons learned. Coast. Eng. J. 57, 1540001. https://doi.org/10.1142/S057856341540001X.
Pawlowicz, R., Beardsley, B., Lentz, S., 2002. Classical tidal harmonic analysis including error estimates in MATLAB using T_TIDE. Comput. Geosci. 28 (8), 929–937.
Poljanšek, K., Marin Ferrer, M., De Groeve, T., Clark, I., (Eds.), 2017. Science for disaster risk management 2017: knowing better and losing less. EUR 28034 EN, Publications Office of the European Union, Luxembourg. ISBN 978-92-79-60679-3. doi:10.2788/842809.
Rose, A., 2004. Economic principles, issues, and research priorities in hazard loss estimation. In: Okuyama, Y., Chang, S.E. (Eds.), Modeling Spatial and Economic Impacts of Disasters. Advances in Spatial Science, Springer, Berlin, Heidelberg.
Sanuy, M., Duo, E., Jäger, W.S., Ciavola, P., Jiménez, J.A., 2018. Linking source with consequences of coastal storm impacts for climate change and risk reduction scenarios for Mediterranean sandy beaches. Nat. Hazards Earth Syst. Sci. 18, 1825–1847. https://doi.org/10.5194/nhess-18-1825-2018.
Scorzini, A., Frank, E., 2017. Flood damage curves: new insights from the 2010 flood in Veneto, Italy. J. Flood Risk Manage. 10, 381–392. https://doi.org/10.1111/jfr3.12163.
Simpson, M.J.R., Nilsen, J.E.Ø., Ravndal, O.R., Breili, K., Sande, H., Kierulf, H.P., Steffen, H., Jansen, E., Carson, M., Vestøl, O., 2015. Sea Level Change for Norway: Past and Present Observations and Projections to 2100. Norwegian Centre for Climate Services report 1/2015. ISSN 2387-3027. Oslo, Norway.
Simpson, M., Breili, K., Kierulf, H. P., Lysaker, D., Ouassou, M., Haug, E., 2012. Estimates of Future Sea-Level Changes for Norway. Technical Report of the Norwegian Mapping Authority.
Simpson, M.J.R., Ravndal, O.R., Sande, H., Nilsen, J.E.Ø., Kierulf, H.P., Vestøl, O., Steffen, H., 2017. Projected 21st century sea-level changes, observed sea level extremes, and sea level allowances for Norway. J. Mar. Sci. Eng. 5, 36. https://doi.org/10.3390/jmse5030036.
Viavattene, C., Jiménez, J.A., Ferreira, O., Priest, S., Owen, D., McCall, R., 2018. Selecting coastal hotspots to storm impacts at the regional scale: a Coastal Risk Assessment Framework. Coast. Eng. 134, 33–47. https://doi.org/10.1016/j.coastaleng.2017.09.002.
Viavattene, C., Micou, A. P., Owen, D., Priest, S., Parker, D., 2015. RISC-KIT Documentation – Deliverable D2.2 – Coastal Vulnerability Indicator Library. Available at: http://www.risckit.eu/np4/file/23/RISC_KIT_D.2.2_CVIL_Guidance_Document.pdf (last access: 11 July 2019).
Vousdoukas, M.I., Bouziotas, D., Giardino, A., Bouwer, L.M., Mentaschi, L., Voukouvalas, E., Feyen, L., 2018a. Understanding epistemic uncertainty in large-scale coastal flood risk assessment for present and future climates. Nat. Hazards Earth Syst. Sci. 18, 2127–2142. https://doi.org/10.5194/nhess-18-2127-2018.
Vousdoukas, M.I., Mentaschi, L., Voukouvalas, E., Bianchi, A., Dottori, F., Feyen, L., 2018b. Climatic and socioeconomic controls of future coastal flood risk in Europe. Nat. Clim. Change. 8 (9), 776–780. https://doi.org/10.1038/s41558-018-0260-4.
Vousdoukas, M.I., Voukouvalas, E., Annunziato, A., Giardina, A., Feyen, L., 2016. Projections of extreme storm surge levels along Europe. Clim. Dyn. 47 (9–10), 3171–3190. https://doi.org/10.1007/s00382-016-3019-5.
Wagenaar, D.J., de Bruijn, K.M., Bouwer, L.M., de Moel, H., 2016. Uncertainty in flood damage estimates and its potential effect on investment decisions. Nat. Hazards Earth Syst. Sci. 16, 1–14. https://doi.org/10.5194/nhess-16-1-2016.
Weigel, A. P., 2012. Ensemble forecasts . In: Jolliffe, I.T., Stephenson. D.B. (eds.), Forecast Verification: A Practitioner's Guide in Atmospheric Science. JohnWiley & Sons, Ltd. Chichester, UK. https://doi.org/10.1002/9781119960003.ch8.